

Effects of antistatic agent on the mechanical, morphological and antistatic properties of polypropylene/organo-montmorillonite nanocomposites

W. S. Chow*, W. L. Tham

School of Materials and Mineral Resources Engineering, Engineering Campus, Universiti Sains Malaysia, 14300 Penang, Malaysia

Received 25 November 2008; accepted in revised form 9 January 2009

Abstract. Polypropylene (PP) and PP/organo-montmorillonite (OMMT) compounds containing antistatic agent (3, 6 and 9 wt%) were prepared using co-rotating twin screw extruder followed by injection molding. PP/OMMT composites were prepared by mixing of PP, OMMT and maleated PP (PPgMAH). The mechanical properties of PP blends and PP/OMMT nanocomposites were studied by tensile and impact tests. The effect of antistatic agent (AA) on the surface resistivity of PP and PP/OMMT nanocomposites were studied. The morphological properties of PP blends and PP/OMMT nanocomposites were characterized by using field emission scanning electron microscopy (FESEM). The intercalation of OMMT silicates layer in PP nanocomposites was characterized using X-ray diffraction (XRD). The impact strength of PP blends and PP/OMMT nanocomposites did not vary significantly by the addition of antistatic agent. The tensile modulus and tensile strength of PP/OMMT nanocomposites were slightly decreased with the increasing loading of antistatic agents. From FESEM analysis, the dispersion of antistatic agent in the PP matrix can be revealed. In addition, the surface resistivity of PP/OMMT compound was affected by the loading of antistatic agent. XRD results indicated the formation of intercalated nanocomposites for PP/OMMT/AA.

Keywords: *nanocomposites, polypropylene, organo-montmorillonite, antistatic agent, material testing*

1. Introduction

Nowadays, plastics have replaced metals and become the material of choice in electronic components because they have higher flexibility, lighter weight, better colorability and higher cost effectiveness [1, 2]. The function of antistatic agent is to prevent the build-up of static electrical charge due to the transfer of electrons to the material surface. Electrostatic charging of composites can lead dust deposition, electric shocks and damages in electronic equipment [3]. Antistatic agent is able to dissipate or promote the decay of static electricity. In addition, an antistatic agent could improve processability, mold release, and give better internal and

external lubrication. The antistatic agents are general ‘soap like’ molecules with a hydrophobic and a hydrophilic part. The hydrophilic part may consist of fatty acid esters, ethoxylated amine and phosphate esters which can migrate to the surface and attract a layer of water. This could lead to the enhancement of surface conductivity of a polymeric material [3]. The main function of the antistatic agent is to promote a conductive channel. A continuous water layer will be formed due to the attachment of vapor to the surface of the antistatic agent. The conductivity of the water layer increased when the number of ions increases, resulting in better antistatic properties of the polymeric materials [4–5].

*Corresponding author, e-mail: chowwenshyang@yahoo.com
© BME-PT and GTE

Polypropylene (PP) is one of the most widely used polyolefin polymers because of its low cost, low density and high specific properties. The PP blends and composites find wide application in automotive parts, extruded profiles, cable insulation, footwear, and packaging industry. Clay minerals are composed of silicate layers with the fundamental unit in 1 nm thickness planar structure [6]. Montmorillonite (MMT) is a valuable mineral and is widely used in many industrial applications because of its high aspect ratio, plate morphology, natural abundance and cost effectiveness. The expandable layered silicates of MMT can be intercalated and/or exfoliated by polymer chain to form nanocomposites [7]. The dispersion of organically modified layered silicates (organoclay) in PP induces enhancement in mechanical properties, flame resistance, heat distortion temperature and barrier properties. Furthermore, these improvements are achieved at clay loadings as low as 5 wt% [8, 9]. For non-polar polymers such as polyethylene (PE) and PP, the interaction between polymer chains and MMT surface is relatively weak and the polymer chains are difficult to intercalate into MMT. Therefore, compatibilizers were often added to increase the degree of interaction between polymer chains and MMT [10, 11]. The properties improvement of nanocomposites is correlated with the intercalation/exfoliation and dispersion of clay layer silicate in polymer matrix. Exfoliation of polymer in layered silicate depends on several factors such as types of clay, organic modifier, and polymer matrix [12, 13]. In general, for PP/clay nanocomposites, a functionalized polymer such as PP grafted with maleic anhydride (PPgMAH) is added to improve the interfacial interaction and compatibility between PP and clays. It is believed that the enhancement of the PP properties depends on the molecular weight and grafting degree of PPgMAH and the relative ratio of PPgMAH/clay. Low grafting percentage of PPgMAH (typically 0.5–2%) hardly enhances the compatibility significantly. While, too much of PPgMAH may lead to the deterioration of nanocomposites properties [14].

In this work, the PP/OMMT compounds were first prepared by melt blending of PP, OMMT and PPgMAH. The aim of this study is to evaluate the effect of antistatic agent on the mechanical properties, morphology and surface resistivity of PP/OMMT nanocomposites. It is believed that the

antistatic agent can be intercalated into the inter-layer spacing of OMMT silicate layers, and thus reduce the migration of antistatic agent from the PP nanocomposites. As a result, the antistatic effects can be maintained for a longer time.

2. Experimental

2.1. Materials

PP copolymer (SM240) was supplied by Titan (M) Sdn Bhd. The MFI and density of PP is 25 g/10 min and 0.9 g/cm³, respectively. The OMMT (1.30P) was supplied by Nanocor, USA. PPgMAH with a percentage of MAH 1.47% was supplied by Eastman Chemical, USA. The antistatic agent (Irgastat P 18) based on polyamide/polyether block amide was supplied by Ciba Specialty Chemical (M) Sdn Bhd. PP containing 3, 6, and 9 wt% of antistatic agent (AA) is designated as PP/AA3, PP/AA6 and PP/AA9, respectively. PP/OMMT compounds [denoted as (PP/OMMT)MB] were first prepared by mixing PP, OMMT and PPgMAH at a ratio of 87:3:10. The PP/OMMT nanocomposites containing 3, 6, and 9 wt% of AA is labeled as PP/OMMT/AA3, PP/OMMT/AA6 and PP/OMMT/AA9, respectively.

2.2. Preparation of PP nanocomposites

2.2.1. Co-rotating twin-screw extrusion

Prior to extrusion, OMMT, PPgMAH and antistatic agent were dried in an oven for 3 hours at 80°C. The extrusion processes of PP/AA blends and PP/OMMT/AA composites were carried out using a co-rotating twin screw extruder (model PSM 30, Sino Alloy, Taiwan) with a *L/D* 40 and intermeshing screw configuration. The screw speed was set at 150 rpm. The processing temperature was set in the range of 155–175°C. Further, the PP/OMMT/AA composites were prepared by mixing (PP/OMMT) MB with the antistatic agent at three different loadings, i.e. 3, 6 and 9 wt%.

2.2.2. Mini vertical injection molding

The PP samples were prepared by using a mini vertical injection molding (model RR/TSMP, Ray-Ran Test Equipment LTD, United Kingdom). The barrel temperature was set in the range of 180–185°C. The mold temperature was set at 80°C.

2.3. Materials characterization

2.3.1. Tensile tests

The samples were prepared by compression molding method. Dumbbell specimens were cut from 1 mm thickness compression-molded sheet. Tensile test was carried out with an Instron tensile machine (model 3366, USA) at 27°C (50% relative humidity), according to ASTM D638, at a crosshead speed of 50 mm/min. Tensile modulus, tensile strength and elongation at break of the PP samples were evaluated from the stress-strain data.

2.3.2. Impact tests

The Charpy impact strength of PP samples was determined according to ASTM D5942 by using a pendulum impact machine (Zwick, USA). The Charpy impact tests were done for both un-notched and single-notched specimens at room temperature. A pendulum with 7.5 J was selected for the impact tests. For unnotched specimen, the Charpy impact strength (a_{cU}), was calculated using Equation (1). For single-notched specimens, the Charpy impact strength (a_{cN}) was calculated using Equation (2):

$$a_{cU} = \frac{W}{h \cdot b} \cdot 10^{-3} \quad (1)$$

$$a_{cN} = \frac{W}{h \cdot b_N} \cdot 10^{-3} \quad (2)$$

where W – corrected energy absorbed by breaking the test specimen [J], h – thickness of the test specimen [mm], b – width of the test specimen [mm], b_N – remaining width at the notch base of the test specimen [mm].

2.3.3. Field emission scanning electron microscopy (FESEM)

The fracture surface of PP/OMMT composites was investigated using a field emission scanning electron microscopy (FESEM, Zeiss Supra 35VP) at an accelerator voltage of 15 kV. The fracture surface of the PP specimens was sputter-coated with a thin gold-palladium layer in vacuum chamber for conductivity before examination.

2.3.4. X-ray diffraction (XRD)

X-ray diffraction (XRD) analyses of OMMT, (PP/OMMT)MB and PP/OMMT/AA composites were performed on a Siemens Diffractometer D5000 machine (Germany) using $\text{CuK}\alpha$ radiation. The samples were scanned in a fixed step size, 0.040° with a step time of 10 s in the range of $2\text{--}10^\circ$. The d-spacing (d) of the interlayer gallery of OMMT and the PP/OMMT nanocomposites was calculated by using Bragg's Law (c.f. Equation (3)):

$$n\lambda = 2d \sin\theta \quad (3)$$

2.3.5. Surface resistivity tests

Surface resistivity tests of the PP samples were carried out according to ASTM D-257-99 using Advantest R8340 Ultra High Resistance Meter. The surface resistivity of PP composites (before and after exposure to room temperature for 3–6 months) was determined by using Equation (4). The thickness of specimen, test voltage and test time is 1mm, 500 V and 1 min, respectively (Equation (4)):

$$\rho_s = \frac{\pi(D+d)}{D-d} \cdot R_s \quad (4)$$

where, ρ_s – surface resistivity [ohm/sq], R_s – surface resistance [ohm], π – ratio of the circumference of a circle to its diameter equal with 3.14, D – inside diameter of guard electrode [cm], d – diameter of main electrode [cm].

3. Results and discussion

3.1. Tensile properties

Figure 1 shows the effect of antistatic agents (AA) on the tensile modulus of PP and (PP/OMMT)MB. The tensile modulus of PP was increased by the addition of OMMT. This is due to the reinforcing effects of OMMT layered silicates. According to Ding *et al.* [15], the uniformly dispersed MMT tactoid with intercalated structures could significantly increase the mechanical properties of a polymer composite even at a low content of OMMT fillers. The OMMT filler could influence the orientation of

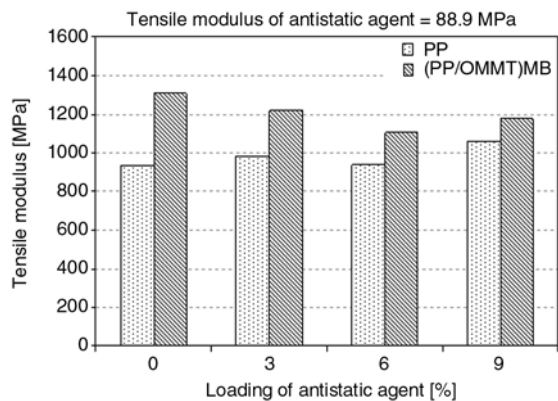


Figure 1. Effect of antistatic agents (AA) on the tensile modulus of PP and (PP/OMMT)MB composites

the lamella in the polymer crystalline [16]. The increment of degree of crystallinity could lead to the enhancement of stiffness and modulus of the PP. Similar observation also reported for various different types of polymer/clay nanocomposites. The tensile modulus of polyamide 6/polypropylene (PA6/PP) blend was increased by the addition of organoclay. This is due to high stiffness of silicate layers, the large aspect ratio and surface area of silicate layers and constraining effect of these layers on molecular motion of polymer chains [17, 18]. In Figure 1, it can be also observed that the tensile modulus of PP was slightly increased by the addition of antistatic agent compare to pure PP. However, the increments of tensile modulus are not significant between PP and PP/AA. The tensile modulus of (PP/OMMT)MB was decreased by the addition of antistatic agents. Note that the tensile modulus of antistatic agent is 88.9 MPa. The antistatic agent is more flexible than (PP/OMMT)MB. Thus, the addition of antistatic agents could lead to the reduction of tensile modulus of PP/OMMT composites. According to Kusmono *et al.* [17], the

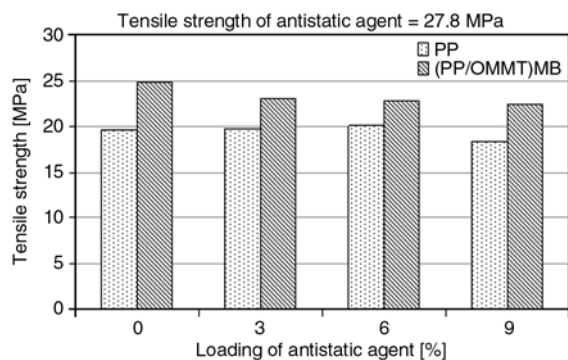


Figure 2. Effect of antistatic agents (AA) on the tensile strength of PP and (PP/OMMT)MB composites

tensile modulus of PA6/PP nanocomposites was reduced by the addition of SEBS-g-MA due to the elastomeric nature of the SEBS-g-MA. Figure 2 shows the effect of antistatic agents (AA) on the tensile strength of PP and (PP/OMMT)MB. The tensile strength of (PP/OMMT)MB is relatively higher than that of PP. This is attributed to the improved interfacial interaction between PP and OMMT in the presence of PPgMAH. According to Mishra *et al.* [19], the intercalation of polymer chain inside silicate layers leads to an increase in the surface area of interaction between clay and polymer matrix. Hence, the tensile strength of the nanocomposite increases slightly as compared to the pristine equivalent. The tensile strength of PP/AA blends (3–9% of AA) is comparable to neat PP. It can be observed that the antistatic agents did not influence much the mechanical properties of PP. The tensile strength of (PP/OMMT)MB was slightly decreased by the addition of antistatic agents. This is attributed to the high flexibility and plasticization effects of antistatic agent. Figure 3 shows the effect of antistatic agents (AA) loading on the elongation at break of PP and (PP/OMMT)MB. The elongation at break for (PP/OMMT)MB composite is lower than that of pure PP. The loading of filler may increase the stress concentration and causes the composite to fail in a brittle manner as compared to PP [20, 21]. The elongation at break of (PP/OMMT)MB was not influenced by the addition of antistatic agent. Thus, it is believed that the antistatic agents’ main function is to dissipate static electric charge accumulated on the surface of plastic, rather than to alter the mechanical properties of a plastic. However, the elongation at break of PP was slightly decreased by the addition of antistatic

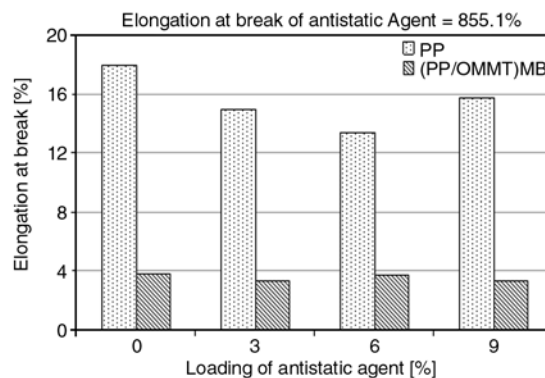


Figure 3. Effect of antistatic agents (AA) on the elongation at break of PP and (PP/OMMT)MB composites

agent. According to Li *et al.* [3], phase separation occurred between the AA and PP matrix during co-spinning process. The AA forms the antistatic mechanism with polymer, the polar radical groups (e.g. C–O–C, –OH and SO₃Na) attract atmospheric moisture and transfer moisture from the polymer surface to inner AA phases. The charge transmission path of AA in polymer matrix is formed by the network of AA phases, and result in dissipation of static charges. When the content of antistatic agent is increased, more transmission paths are formed. The build of transmission paths of AA in PP may restrict the movement of polymer chains and consequently reduce the elongation at break of PP.

3.2. Impact properties

The effect of antistatic agents (AA) on the un-notched Charpy impact strength of PP and (PP/OMMT)MB composite is shown in Figure 4. It can be seen that the loading of antistatic agents (e.g. 3, 6 and 9%) do not affect the impact strength of PP. The impact strength of PP/AA is comparable with neat PP. The impact strength of PP was slightly reduced by the addition of OMMT. According to Ding *et al.*, [15], the OMMT was dispersed in the PP matrix on the nanometer scale and part of the OMMT was intercalated by PP chains. Thus, the OMMT layered silicates may confine the segmental movement of PP macromolecules. However, the impact strength of (PP/OMMT)MB is comparable to the neat PP. This is attributed to the PPgMAH component that can improve the interfacial interaction between PP and OMMT. A better interfacial interaction could lead to improvement of impact strength with high absorption energy during

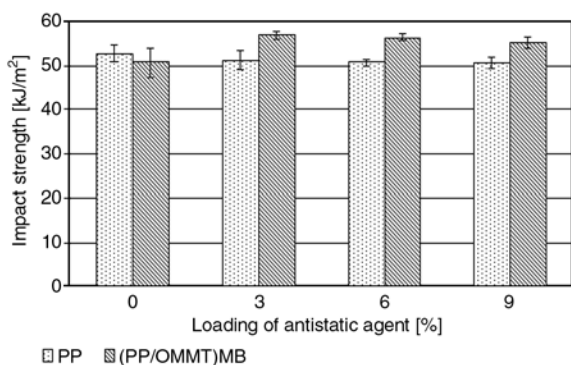


Figure 4. Effect of antistatic agents (AA) on the un-notched Charpy impact strength of PP and (PP/OMMT)MB composites

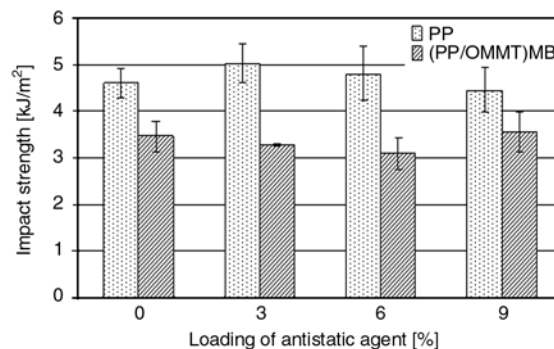


Figure 5. Effect of antistatic agents (AA) on the notched Charpy impact strength of PP and (PP/OMMT)MB composites

impact deformation. According to Kusmono *et al.* [17], the high impact strength of PA6/PP/OMMT could be attributed to the improved interfacial interaction resulting from the formation of maleic anhydride grafted styrene-ethylene-butylene-styrene (SEBS-g-MA) in the composites. It is interesting to note that the impact strength of (PP/OMMT)MB was slightly increased by the addition of antistatic agent. This is due to the flexibility and ductility characteristics of the antistatic agent. Accordingly, the PP/OMMT/AA samples will absorb more energy during impact deformation. According to Cai *et al.* [20], the grafted polymer might play the role of a bumper interlayer around the filler, while absorbing impact energy and preventing initiation of cracks. A further improvement of nanocomposites' ductility is exhibited as an increase in flexibility of the grafted polymer chains. Figure 5 shows the effect of antistatic agents on notched Charpy impact strength of PP and (PP/OMMT)MB composite. The different loading of antistatic agents in PP and (PP/OMMT)MB do not show any alteration on impact strength obviously. However, the PP/AA blends exhibited higher impact strength compared to PP/OMMT/AA composites. The notched samples were fractured easily compared to the un-notched ones. The value of impact strength for notched samples decrease rapidly compared to un-notched samples, especially for (PP/OMMT)MB nanocomposite. This may be due to the dispersed and intercalated OMMT layer silicates in the PP matrix which could restrict the segmental movement of PP macromolecules and further decrease its impact strength [19].

Table 1. Interlayer spacing and surface resistivity of PP and (PP/OMMT)MB

Materials designation	2θ	d_{001} [nm]	Surface resistivity [ohm/sq]			Category
			control	3 months	6 months	
AA	–	–	10^8	10^8	10^8	antistatic
PP	–	–	$>10^{12}$	$>10^{12}$	$>10^{12}$	insulator
PP/AA3	–	–	$>10^{12}$	$>10^{12}$	$>10^{12}$	insulator
PP/AA6	–	–	10^{11}	10^{11}	10^{11}	antistatic
PP/AA9	–	–	10^{11}	10^{11}	10^{11}	antistatic
OMMT	3.32	2.66	10^8	10^8	10^8	–
PP/OMMT	3.24	2.72	$>10^{12}$	$>10^{12}$	$>10^{12}$	insulator
PP/OMMT/AA3	3.22	2.74	$>10^{12}$	$>10^{12}$	$>10^{12}$	insulator
PP/OMMT/AA6	3.20	2.76	$>10^{12}$	$>10^{12}$	$>10^{12}$	insulator
PP/OMMT/AA9	3.18	2.77	10^{11}	10^{11}	10^{11}	antistatic

3.3. Surface resistivity

Table 1 shows the effect of antistatic agent (AA) on the surface resistivity of PP before and after exposure to room temperature for 3–6 months. It can be seen that the surface resistivity of all the samples remained unchanged for the duration of 6 months. The surface resistivity of antistatic agent is about 10^8 ohm/sq. Neat PP and PP/AA3 with 10^{12} ohm/sq surface resistivity was in the category of insulator materials. However, the surface resistivity of PP/AA6 and PP/AA9 blends was recorded at 10^{11} ohm/sq. This indicates that both of the PP/AA6 and PP/AA9 could be categorized as antistatic materials. The surface resistivity of PP/AA6 and PP/AA9 were decreased by the incorporation of antistatic agent. However, PP/AA3 did not show significant changing of surface resistivity because the content of antistatic agent unable imparts antistatic properties on PP. Accordingly the probability of migration for the hydrophilic groups to the material surface to attract water is low. Table 1 also shows the effect of antistatic agent (AA) on the surface resistivity of (PP/OMMT)MB composites. Surface resistivity of PP/OMMT, (PP/OMMT)/AA3 and (PP/OMMT)/AA6 are more than 10^{12} ohm/sq, while (PP/OMMT)/AA9 showed the surface resistivity of 10^{11} ohm/sq. It is worth noting that the surface resistivity of PP/OMMT/AA9 remained 10^{11} ohm/sq for 6 months. This indicates that (PP/OMMT)/AA9 nanocomposites could exhibits antistatic behaviors. However, PP/OMMT, (PP/OMMT)/AA3 and (PP/OMMT)/AA6 nanocomposites were classified in the insulator category where the surface resistivity recorded at 10^{12} – 10^{16} ohm/sq. (PP/OMMT)/AA3 and (PP/OMMT)/AA6 nanocomposites could not achieve the antistatic behavior; this may be due to the insufficient and

lower content of antistatic agent. In addition, it is believed that the antistatic agent could intercalate into the OMMT silicate layers. This will reduce the possibility of antistatic agent migrate to the PP sample surface. One may believe that an optimum migration rate has to be achieved in order to facilitate the migration of neighbor's antistatic agent to the surface from the bulk, but it should not lose the whole amount of antistatic agent too fast. On the other hand, when 9% antistatic agent added in PP/OMMT, it is able to give the antistatic ability due to the migration of antistatic agent to the PP composites surface. According to Ratnayake and Haworth [22], the water contact angles were increased dramatically by adding clay into PP/antistatic agent blends. This is because most of functional group of antistatic agent interacts with clay particles, rather than migrating onto the surface, especially at low concentration of antistatic agent.

3.4. X-ray diffraction (XRD)

The 2θ and d-spacing of OMMT and (PP/OMMT)MB with and without AA was shown in Table 1. The (PP/OMMT)MB nanocomposite shows a small shoulder which appeared at $2\theta = 3.24^\circ$. The corresponding d-spacing of (PP/OMMT)MB is $d_{001} = 2.72$ nm. This is due to the intercalation of clay layers by the addition of PPgMAH. According to Bertini *et al.* [23], the patterns of the PP/OMMT composite provides direct evidence of the intercalation. A shoulder shifted to lower diffraction angles of 2θ with the presence of montmorillonite. A higher content of PPgMAH improves the intercalation and clay dispersability in the PP matrix [22]. Interesting to note that, the d_{001} peak of PP/OMMT has been broadened by the addition of antistatic

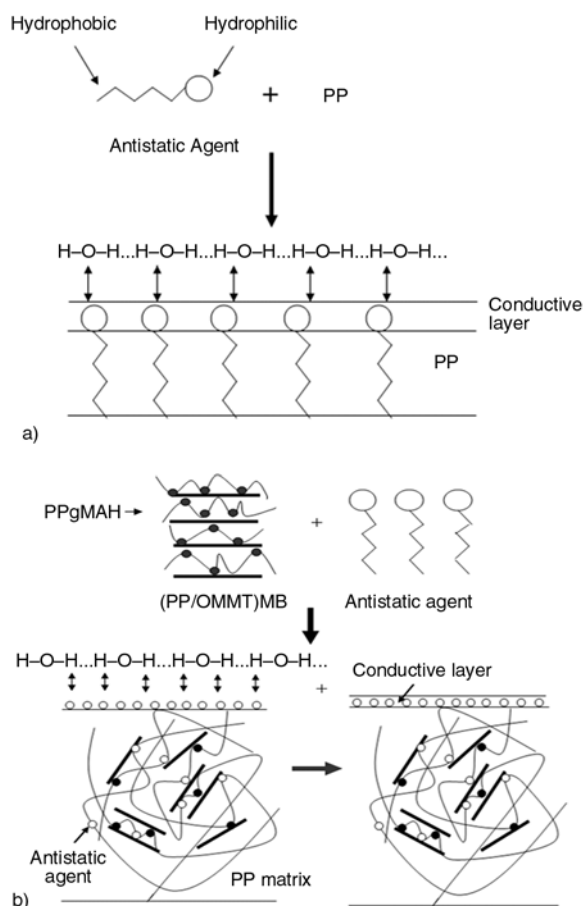


Figure 6. a – Possible interaction mechanism between PP and AA, b – Possible interaction and intercalation mechanism of PP/OMMT/AA nanocomposites

agent. Thus, it is believed that the antistatic agent is able to intercalate into the clay interlayer gallery. It can be seen that the d -spacing of (PP/OMMT)MB increased with the increasing concentration of AA. The PP/OMMT/AA9 shows a $2\theta = 3.18^\circ$, which is corresponding to the d -spacing of 2.78 nm. According to Ratnayake and Haworth [22], the XRD results clearly show that the shifting of peaks to a lower Bragg angle as the loading of antistatic agent (AA) in PP/OMMT composites increasing. They also reported that by the addition of 0.5% (by weight) of AA in composite, the highest interlayer spacing was achieved. However, a further increase of additive concentration in composite is not effective in modifying the interlayer spacing, probably because of the migration of additional antistatic agent additive onto the surface. From Table 1, it can be seen that the intercalation and exfoliation of OMMT layered silicate in PP composites could be correlated to the surface resistivity of the composites. For the PP/OMMT/AA9, when d_{001} value of

the interlayer spacing is sufficient, it is possible for the excess amount of AA to migrate to the materials surface and thus provide the antistatic characteristics. Figure 6a shows the possible interaction mechanism between PP and AA. It can be seen that the AA can migrate to the PP surface to form a conductive layer. Figure 6b shows the possible interaction and intercalation mechanism in PP/OMMT/AA nanocomposites. Note that the low molecular weight AA can intercalate into the OMMT layer silicate. If the amount of AA is sufficient, in addition to the intercalation of AA, it is believed that some amount of the AA can migrate to the PP surface and form a conductive layer.

3.5. Field emission scanning electron microscopy (FESEM)

Figure 7a shows the FESEM micrographs taken from the impact fractured surface of neat PP. Figure 7b shows the FESEM micrographs taken from the impact fractured surface of PP/AA blends. There were two types of small particles observed from the sample fractured surface. It can be seen that some particles (shown by pink arrow in Figure 7b) are in the range of 5 to 6 μm which can be observed in Figure 7a as well. Recall that the PP used in this study is a type of PP copolymer that contains ethylene and propylene. The ethylene is distributed and dispersed in the PP matrix. Hence, the small particles protruded on the fractured surface of PP matrix could be assigned to ethylene. Besides, there are lots of small particles about 0.5–1.0 (shown by orange arrow in Figure 7b) were also observed on the fractured plane. It is believed that the small particles present on the fracture surface of PP/AA correspond to the antistatic agent. Figures 7c and 7d shows the FESEM micrographs taken from the impact fractured surface of PP/OMMT and PP/OMMT/AA composites. Particle shown by blue arrow could correspond to OMMT. EDX was used to confirm the OMMT elements. Figure 8 shows the EDX spectra taken from PP/OMMT/AA (c.f. Figure 7d), there were 5 elements can be observed, i.e. C, O, Si, Na and Ca. According to Chow *et al.* [24], the carbon is due to the octadecylamine intercalant used. O, Si, Na and Ca elements represent components of OMMT. From the FESEM micrograph taken from the PP/OMMT/AA nanocomposites, note that the anti-

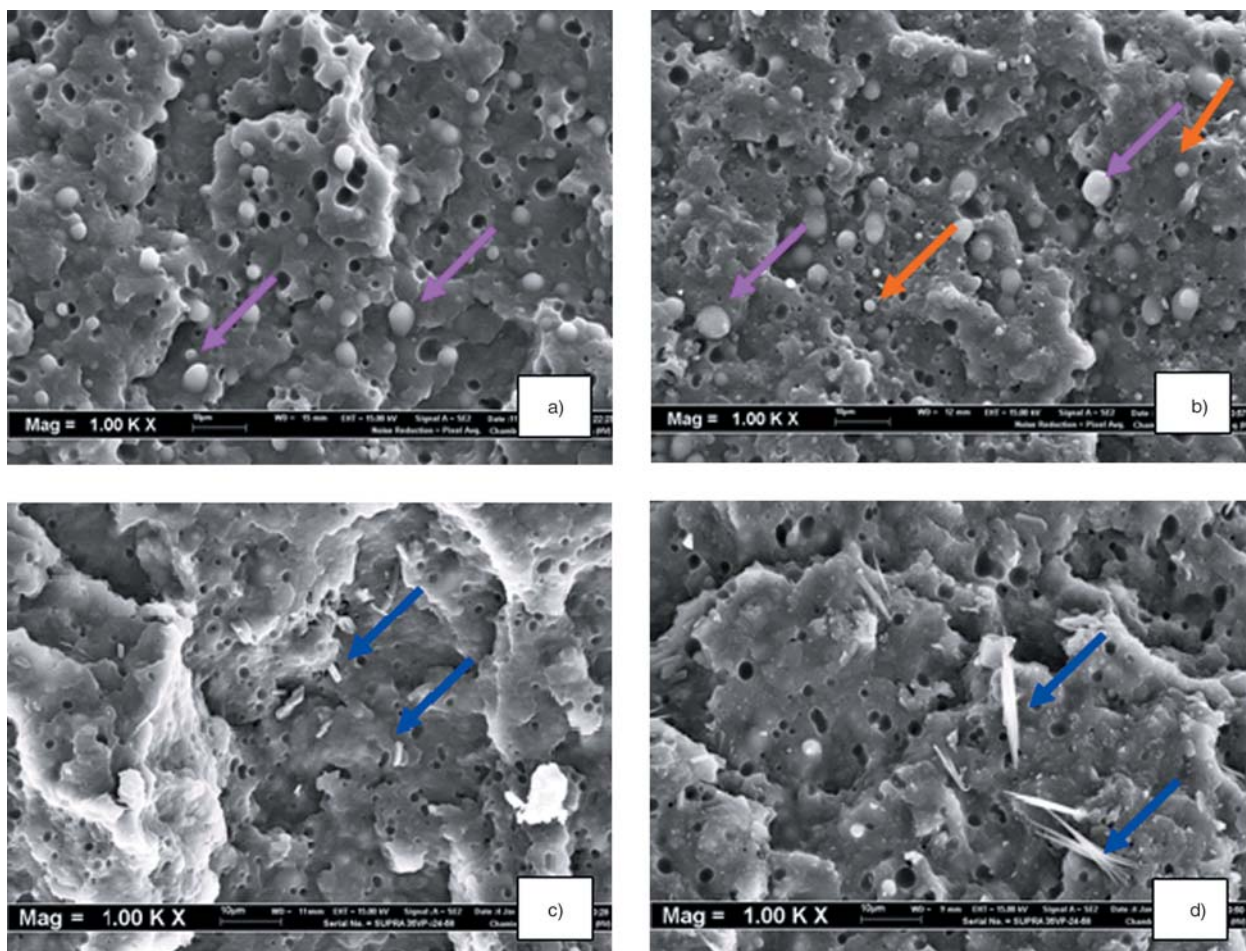


Figure 7. a – FESEM micrographs taken from the impact fractured surface of PP, b – FESEM micrographs taken from the impact fractured surface of PP/AA blends, c – FESEM micrographs taken from the impact fractured surface of PP/OMMT composites, d – FESEM micrographs taken from the impact fractured surface of PP/OMMT/AA composites

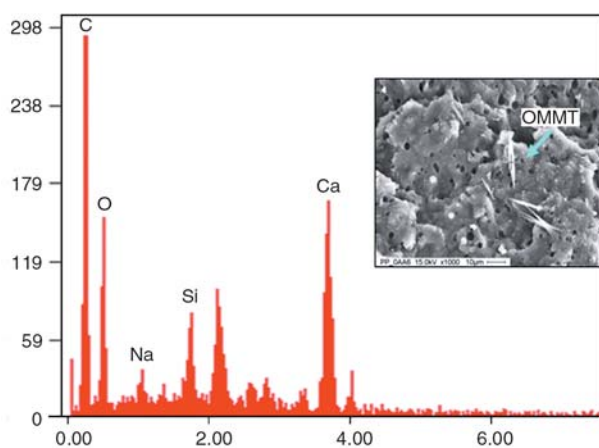


Figure 8. EDX spectra taken from the PP/OMMT/AA nanocomposites

static agent particles could not be observed on the fractured surface. According to Ratnayake and Haworth [22], they suggested that functional slip additives and antistatic agent will intercalate into clay galleries. They observed through TEM micro-

graph, clay particles are separated into much smaller stacks and dispersed homogenously throughout the PP matrix when antistatic agent and PPgMAH are added. It can be attributed to the co-intercalation of AA with PPgMAH that will increase the clay dispersibility in PP matrix. Therefore, the wettability and intercalation capability of nanocomposites increases with the increasing of the polarity in PPgMAH and antistatic agent.

4. Conclusions

This study reveals the effects of antistatic agent (AA) on the mechanical properties, morphology and surface resistivity of PP and (PP/OMMT)MB nanocomposites. The AA only give minor effects (or in some case, insignificant effects) on the tensile modulus, strength, elongation at break and impact strength (notched and un-notched) of the PP and (PP/OMMT)MB nanocomposites. The incor-

poration of AA and PPGMAH may provide better wettability and interfacial interaction between OMMT and PP matrix. The surface resistivity of the PP/OMMT nanocomposites could be correlated to the concentration of AA and intercalation/exfoliation-ability of the OMMT. It is hypothesized that the AA could be intercalated into the OMMT layered silicates which could influence the surface resistivity of the PP and its nanocomposites. It is worth to note that the surface resistivity of PP/OMMT/AA9 was remained 10^{11} ohm/sq even after exposure to room temperature for 6 months.

Acknowledgements

W. S. Chow would like to thank Universiti Sains Malaysia for the USM Short Term Grant financial support for this research project.

References

- [1] Harper C. A.: Modern plastics handbook. McGraw-Hill, New York (1999).
- [2] Amarasekera J.: Conductive plastics for electrical and electronic applications. Reinforced Plastics, **49**, 38–41 (2005).
DOI: [10.1016/S0034-3617\(05\)70734-7](https://doi.org/10.1016/S0034-3617(05)70734-7)
- [3] Li C., Liang T., Lu W., Tang C., Hu X., Cao M., Liang J.: Improving the antistatic ability of polypropylene fibers by inner antistatic agent filled with carbon nanotubes. Composites Science and Technology, **64**, 2089–2096 (2004).
DOI: [10.1016/j.compscitech.2004.03.010](https://doi.org/10.1016/j.compscitech.2004.03.010)
- [4] Ma C-C., Chen Y-J., Kuan H-C.: Polystyrene nanocomposites materials: Preparation, morphology, mechanical, electrical and thermal properties. Journal of Applied Polymer Science, **98**, 2266–2273 (2005).
DOI: [10.1002/app.23221](https://doi.org/10.1002/app.23221)
- [5] Hong C. K., Kim M-J., Oh S. H., Lee Y-S., Nah C.: Effects of polypropylene-g-(maleic anhydride/styrene) compatibilizer on mechanical and rheological properties of polypropylene/clay nanocomposites. Journal of Industrial and Engineering Chemistry, **14**, 236–242 (2008).
DOI: [10.1016/j.jiec.2007.11.001](https://doi.org/10.1016/j.jiec.2007.11.001)
- [6] Hausman K.: Permanent antistatic agents offers long term performance for films and containers. Plastic, Additives and Compounding, **9**, 40–42 (2007).
DOI: [10.1016/S1464-391X\(07\)70070-3](https://doi.org/10.1016/S1464-391X(07)70070-3)
- [7] Qin H., Zhang S., Zhao C., Feng M., Yang M., Shu Z., Yang S.: Thermal stability and flammability of polypropylene/montmorillonite composites. Polymer Degradation and Stability, **85**, 807–813 (2003).
DOI: [10.1016/j.polymdegradstab.2004.03.014](https://doi.org/10.1016/j.polymdegradstab.2004.03.014)
- [8] Ray S., Okamoto M.: Polymer/layered silicate nanocomposites: A review from preparation to processing. Progress in Polymer Science, **27**, 1539–1641 (2003).
DOI: [10.1016/j.progpolymsci.2003.08.002](https://doi.org/10.1016/j.progpolymsci.2003.08.002)
- [9] Xanthos M.: Functional fillers for plastics. Wiley, Weinheim (2005).
- [10] Shi D., Yu W., Robert Li K. Y., Ke Z., Yin J. H.: An investigation on the dispersion of montmorillonite (MMT) primary particles in PP matrix. European Polymer Journal, **43**, 3250–3257 (2007).
DOI: [10.1016/j.eurpolymj.2007.05.030](https://doi.org/10.1016/j.eurpolymj.2007.05.030)
- [11] Valera-Zaragoza M., Ramírez-Vargas E., Medellín-Rodríguez F. J., Huerta-Martínez B. M.: Thermal stability and flammability properties of heterophasic PP-EP/EVA/organoclay nanocomposites. Polymer Degradation and Stability, **91**, 1319–1325 (2006).
DOI: [10.1016/j.polymdegradstab.2005.08.011](https://doi.org/10.1016/j.polymdegradstab.2005.08.011)
- [12] Imren D., Boztug A., Yilmaz E., Bayram Zengin H.: Viscometric investigation of compatibilization of the poly(vinyl chloride)/poly(ethylene-co-vinyl acetate) blends by terpolymer of maleic anhydride-styrene-vinyl acetate. Journal of Molecular Structure, **891**, 329–332 (2008).
DOI: [10.1016/j.molstruc.2008.04.003](https://doi.org/10.1016/j.molstruc.2008.04.003)
- [13] Rohlmann C. O., Failla M. D., Quinzani L. M.: Linear viscoelasticity and structure of polypropylene-montmorillonite nanocomposites. Polymer, **47**, 7795–7804 (2006).
DOI: [10.1016/j.polymer.2006.08.044](https://doi.org/10.1016/j.polymer.2006.08.044)
- [14] García-López D., Picazo O., Merino J. C., Pastor J. M.: Polypropylene-clay nanocomposites: Effect of compatibilizing agents on clay dispersion. European Polymer Journal, **39**, 945–950 (2003).
DOI: [10.1016/S0014-3057\(02\)00333-6](https://doi.org/10.1016/S0014-3057(02)00333-6)
- [15] Ding C., Jia D. M., He H., Guo B. C., Hing H. Q.: How organo-montmorillonite truly affects the structure and properties of polypropylene. Polymer Testing, **24**, 94–100 (2005).
DOI: [10.1016/j.polymertesting.2004.06.005](https://doi.org/10.1016/j.polymertesting.2004.06.005)
- [16] Osman M. A., Rupp J. E. P., Suter U. W.: Tensile properties of polyethylene-layered silicate nanocomposites. Polymer, **46**, 1653–1660 (2005).
DOI: [10.1016/j.polymer.2004.11.112](https://doi.org/10.1016/j.polymer.2004.11.112)
- [17] Kusmono, Mohd Ishak Z. A., Chow W. S., Takeichi T., Rochmadi: Influence of SEBS-g-MA on morphology, mechanical and thermal properties of PA6/PP/organoclay nanocomposites. European Polymer Journal, **44**, 1023–1039 (2008).
DOI: [10.1016/j.eurpolymj.2008.01.019](https://doi.org/10.1016/j.eurpolymj.2008.01.019)
- [18] Chow W. S., Mohd Ishak Z. A.: Mechanical, morphological and rheological properties of polyamide 6/organo-montmorillonite nanocomposites. Express Polymer Letters, **2**, 77–83 (2007).
DOI: [10.3144/expresspolymlett.2007.14](https://doi.org/10.3144/expresspolymlett.2007.14)

- [19] Mishra J. K., Hwang K-J., Ha C-S.: Preparation, mechanical and rheological properties of a thermoplastic polyolefin (TPO)/organoclay nanocomposite with reference to the effect of maleic anhydride modified polypropylene as a compatibilizer. *Polymer*, **46**, 1995–2002 (2005).
DOI: [10.1016/j.polymer.2004.12.044](https://doi.org/10.1016/j.polymer.2004.12.044)
- [20] Cai L. F., Mai Y. L., Rong M. Z., Ruan W. H., Zhang M. Q.: Interfacial effects in nano-silica/polypropylene composites fabricated by in-situ chemical blowing. *Express Polymer Letters*, **1**, 2–7 (2007).
DOI: [10.3144/expresspolymlett.2007.2](https://doi.org/10.3144/expresspolymlett.2007.2)
- [21] Hull D., Clyde T. W.: *An introduction to composite materials*. Cambridge University Press, Cambridge (1996).
- [22] Ratnayake U. N., Haworth B.: Polypropylene-clay nanocomposites: Influence of low molecular weight polar additives on intercalation and exfoliated behavior. *Polymer Engineering and Science*, **46**, 1008–1015 (2006).
DOI: [10.1002/pen.20573](https://doi.org/10.1002/pen.20573)
- [23] Bertini F., Canetti M., Audisio G., Costa G., Falqui L.: Characterization and thermal degradation of polypropylene-montmorillonite nanocomposites. *Polymer Degradation and Stability*, **91**, 600–605 (2005).
DOI: [10.1016/j.polymdegradstab.2005.02.027](https://doi.org/10.1016/j.polymdegradstab.2005.02.027)
- [24] Chow W. S., Mohd Ishak Z. A., Kanger-Kocsis J., Apostolov A. A., Ishiaku U. S.: Compatibilizing effect of maleated polypropylene on the mechanical properties and morphology of injection molded polyamide 6/polypropylene/organoclay nanocomposites. *Polymer*, **44**, 7427–7440 (2003).
DOI: [10.1016/j.polymer.2003.09.006](https://doi.org/10.1016/j.polymer.2003.09.006)